

## Electronic Supplementary Information (ESI)

### **Porous vanadium-doped titania with active hydrogen: a renewable reductant for chemoselective hydrogenation of nitroarenes at ambient condition**

**Juan Su<sup>†,‡</sup> Xiao-Xin Zou,<sup>†,‡</sup> Guo-Dong Li,<sup>‡</sup> Lu Li,<sup>†,‡</sup> Jun Zhao,<sup>‡</sup> Jie-Sheng Chen<sup>\*†</sup>**

<sup>†</sup> School of Chemistry and Chemical Engineering, Shanghai Jiao Tong University, Shanghai 200240, China

<sup>‡</sup> State Key Laboratory of Inorganic Synthesis and Preparative Chemistry, College of Chemistry, Jilin University, Changchun 130012, China

E-mail: chemcj@sjtu.edu.cn

## Experimental Section

**Preparation of V-TG precursors.** Titanium n-butoxide (20 mL) was dropped into ethylene glycol (170 mL) under vigorous stirring. After a clear solution was formed, an appropriate amount of ammonium metavanadate was added and the mixture was subsequently refluxed at 180 °C for 3 h. After cooling down to room temperature, the yellow V-TG precipitate was washed several times with ethanol and dried at ambient temperature.

**Preparation of V-TiO<sub>2</sub>(H<sup>\*</sup>) reductants.** The V-TG precursor was immersed in water and irradiated with UV light in a water-cooled quartz cylindrical cell. The UV light source was a 150 W high-pressure mercury lamp (main output 313 nm) and the irradiation intensity of the UV-light was about 100 mW/cm<sup>2</sup>. During the irradiation process, gaseous N<sub>2</sub> was bubbled into the reaction system. Through the UV-irradiation, about 1 g of V-TiO<sub>2</sub>(H<sup>\*</sup>) reductant (black blue in color) was obtained from 2 g V-TG precursor (yellow in color). The V-TiO<sub>2</sub>(H<sup>\*</sup>) reductant was air-sensitive because of its reducing nature. To prevent the reductant from oxidization by air, the sample was preserved in water or methanol purged by nitrogen in a sealed vessel.

**Measurements of FT-IR.** The FT-IR measurement was performed in situ and the sample was dried under vacuum before and after exposure to O<sub>2</sub> to avoid the influence of H<sub>2</sub>O, which may come from air or may be in situ generated. First, the H<sub>2</sub>O molecules in the as-prepared V-TiO<sub>2</sub>(H<sup>\*</sup>) sample were removed by evacuation at 100 °C for 1h. Subsequently, in a dry and oxygen-free glove box, the dry V-TiO<sub>2</sub>(H<sup>\*</sup>) solid was closely filled and sealed in an IR cell with two CaF<sub>2</sub> windows (25 mm in diameter and 3 mm in thickness). When the IR spectrum of V-TiO<sub>2</sub>(H<sup>\*</sup>) was obtained, O<sub>2</sub> was injected into the IR cell and the reductant was oxidized to V-TiO<sub>2</sub> solid. After another vacuum drying process as the same as the previous one, the IR spectrum of V-TiO<sub>2</sub> was measured again.

It should be pointed that the vacuum drying processes for the sample before and after exposure to O<sub>2</sub> are identical. Therefore, the obvious decrease of OH IR absorption is attributed to the consumption of protons by O<sub>2</sub>, rather than any other influencing factors, such as overheated treatment.

**Measurements of electron paramagnetic resonance (EPR).** The electron paramagnetic resonance spectra were obtained on a JES-FA 200 EPR spectrometer. The details of the instrumental parameters were as follows: microwave frequency: 9.10 GHz (77 K), 9.45 GHz (room-temperature); central field: 3360 G; scanning width: 8000 G; scanning power: 0.998 mW; scanning temperature: 77 K and room-temperature. For EPR measurement of the V-TiO<sub>2</sub>(H<sup>\*</sup>), the sample was first dried by evacuation at 100 °C for 1h, and then the dry solid sample was sealed in quartz tubes for measurements.

**Measurement of active hydrogen (H<sup>\*</sup>) content in V-TiO<sub>2</sub>(H<sup>\*</sup>).** The quantitative measurement of active hydrogen (H<sup>\*</sup>) content in the as-prepared V-TiO<sub>2</sub>(H<sup>\*</sup>) reductant was performed through redox titration using a nitrobenzene methanol solution (61.7 mmol/L) as the oxidant. The content was calculated according to the equation: C<sub>6</sub>H<sub>5</sub>-NO<sub>2</sub> + 6H<sup>\*</sup> = C<sub>6</sub>H<sub>5</sub>-NH<sub>2</sub> + 2H<sub>2</sub>O. About 0.6 g V-TG was immersed in 20 mL methanol, and the mixture was irradiated with UV-light for 30 min

under vigorous stirring and protection of N<sub>2</sub>. About 0.3 g V-TiO<sub>2</sub>(H\*) reductant material was obtained. Then, a nitrobenzene methanol solution (61.7 mmol/L) was dropped into the irradiated mixture until the black-blue color faded completely. The consumed amount of the nitrobenzene methanol solution for the titration was used to calculate the content of the H\* species in the V-TiO<sub>2</sub>(H\*) reductant, and the molar ratio of H\*/(V+Ti) was used to represent the H\* content of V-TiO<sub>2</sub>(H\*) reductant.

**Redox reactions involving V-TiO<sub>2</sub>(H\*) reductants.** Under the protection of N<sub>2</sub>, a certain amount of an nitroarene compound (0.124 mmol) was added into the mixture of 1.4% V-TiO<sub>2</sub>(H\*) (0.3g) and 20 mL methanol under vigorous stirring at room temperature. After 10 s stirring time, the reaction was terminated through injection of O<sub>2</sub> in place of N<sub>2</sub> because the active hydrogen in V-TiO<sub>2</sub>(H\*) was instantly scavenged by O<sub>2</sub> to stop the reaction. The reduction product was separated from the mixture by centrifugation and then filtered through a 0.22 μm syringe filter for qualitative analysis by LC-MS (liquid chromatography-mass spectrometry) and quantitative analysis by HPLC (high-performance liquid chromatography).

**Renewability of V-TiO<sub>2</sub>(H\*) reductant.** After the V-TiO<sub>2</sub>(H\*) reductant (0.3 g) was fully oxidized, the resulting V-TiO<sub>2</sub> (pink solid) was separated from the redox reaction mixture by centrifugation and washed by methanol for three times. The collected solid was irradiated by UV-light under N<sub>2</sub> protection in the presence of methanol for about 30 min and the V-TiO<sub>2</sub>(H\*) reductant was regenerated. Subsequently, nitrobenzene (0.124 mmol) was added into the mixture to thoroughly oxidize the regenerated V-TiO<sub>2</sub>(H\*) reductant. Such process was repeated more than 20 cycles and no obvious loss of reducing capacity of was observed. For comparison, the regeneration test has also been performed in pure water, and we found that the V-TiO<sub>2</sub>(H\*) could not be regenerated without methanol.

**General characterization.** The powder X-ray diffraction (XRD) patterns were recorded on a Rigaku D/Max 2550 X-ray diffractometer with Cu Kα radiation (λ = 1.5418 Å). The X-ray photoelectron spectroscopy (XPS) was performed on an ESCALAB 250 X-ray photoelectron spectrometer with a monochromatized X-ray source (Al Kα hv = 1486.6 eV). The energy scale of the spectrometer was calibrated using Au 4f<sub>7/2</sub>, Cu 2p<sub>3/2</sub>, and Ag 3d<sub>5/2</sub> peak positions. The standard deviation for the binding energy (BE) values is 0.1 eV. The scanning electron microscopic (SEM) images were taken on a JEOL JSM 6700F electron microscope, whereas the FT-IR spectra were acquired on a Bruker IFS 66v/S FT-IR spectrometer. The Raman spectra were obtained with a Renishaw Raman system model 1000 spectrometer with a 20 mW air-cooled argon ion laser (514.5 nm) as the exciting source (the laser power at the sample position was typically 400 μW with an average spot size of 1 μm in diameter). The ICP elemental analyses were performed on a Perkin-Elmer Optima 3300DV ICP spectrometer. The electron paramagnetic resonance (EPR) spectra were recorded on a JES-FA 200 ESR spectrometer. The nitrogen adsorption and desorption isotherms were measured using a Micromeritics ASAP 2020M system, whereas the TEM image was obtained on a JEOL JSM-3010 TEM microscope. A superconducting quantum interference device magnetometer (Quantum Design, MPMS-XL) was used for the magnetic property measurements. The qualitative analysis of the organic species was performed on a liquid

chromatograph (UltiMate 3000) combined with a mass spectrometer (HCTplus<sup>TM</sup>), and the quantitative analysis was on an UltiMate 3000 high-performance liquid chromatograph by using benzene as an internal standard. The analysis of the oxidation products of the sacrifier (methanol) was performed on a Shimadzu GC-2014C gas chromatograph.

### Supporting characterization of V-TG precursors and V-TiO<sub>2</sub>(H\*) reductants

To elucidate the nature of the doped vanadium species, we first investigated the vanadium-doped titanium glycolates (V-TG) precursors. Both the XPS (Fig. S3) and EPR (Fig. S4b,d) data reveal that the doped vanadium is V<sup>4+</sup>.<sup>[S1,S2]</sup> In addition, the XRD results (Fig. S1) show that the V-doping decreases the intensity of the characteristic peak at about 12.5° associated with the (200) crystallographic plane. The crystal structure (Fig. S5) of the V-TG precursor is identical with that of the un-doped titanium glycolate, which is composed of infinite metal alkoxide chains packed together through a van der Waals interaction.<sup>[S3]</sup> It is presumed that the V<sup>4+</sup> ions are doped into the lattice by replacement of Ti<sup>4+</sup> sites, reducing the interactions between the one-dimensional chains and leading to the growth inhibition of (200) crystallographic plane along the direction perpendicular to the *c* axis. This observation is in agreement with the scanning electron microscopic (SEM) images (Fig. S2) which show obvious difference of morphology before and after doping.

More evidence for the nature of the doped V species can be provided by characterizing V-TiO<sub>2</sub> because V-TiO<sub>2</sub>(H\*) reductant is air-sensitive and V-TiO<sub>2</sub> as the oxidization product of V-TiO<sub>2</sub>(H\*) was used to represent the reductant for a series of characterizations (XRD, Raman, TEM, XPS, N<sub>2</sub> adsorption/desorption isotherms and the BJH pore-size distribution) in air. In addition, it was noted that the mass of the V-TiO<sub>2</sub>(H\*) reductant was almost identical to that of its oxidization product V-TiO<sub>2</sub>. As the content of vanadium increases from 0 to 1.9%, the Ti 2p<sub>1/2</sub> peak shifts from 464.6 to 564.4 eV, and the Ti 2p<sub>3/2</sub> signal shifts from 459.0 to 458.7 eV. It is noted that the doping of vanadium affects the morphology and pore feature of the TiO<sub>2</sub>(H\*) material to a certain degree. The TEM image (Fig. S10) and the N<sub>2</sub> adsorption/desorption isotherms (Fig. S11a) (characteristic type-IV curves with H1-type hysteresis loops) demonstrate the porous structure of the samples. The pore size is widened as increasing the vanadium-doping content (Fig. S11b, Table S1). Based on the above results, it is concluded that V species (V<sup>4+</sup>) have been doped in the lattice of V-TG and its derived V-TiO<sub>2</sub>. The fact that after further reduction treatment of the V-TiO<sub>2</sub> material no V<sup>4+</sup> signal is present for the sample suggests that the V<sup>4+</sup> species are located on the (internal and external) surface of the porous V-titania material and are highly accessible to guest molecules such as O<sub>2</sub> and methanol. (Fig. 2b, line 1)

[S1] A. Vadivel Murugan, C. W. Kwon, G. Campet, B. B. Kale, A. B. Mandale, S. R. Sainker, Chinnakonda S. Gopinath, K. Vijayamohanan, *J. Phys. Chem. B*, 2004, **108**, 10736.

[S2] I. L. Moudrakovski, A. Sayari, *J. Phys. Chem.* 1994, **98**, 10895; B. Z. Tian, C. Z. Li, F. Gu, H. B. Jiang, Y. J. Hu, J. L. Zhang, *Chem. Eng. J.* 2009, **151**, 220.

[S3] D. Wang, R. Yu, N. Kumada, N. Kinomura, *Chem. Mater.*, 1999, **11**, 2008.

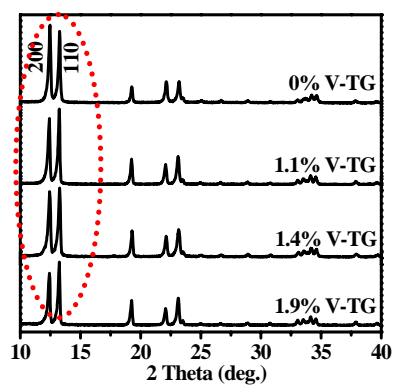


**Fig. S1.** Powder X-ray diffraction patterns of V-TG precursors with different vanadium contents (in red circle, the characteristic peaks are associated with the (200) and (110) crystallographic planes).

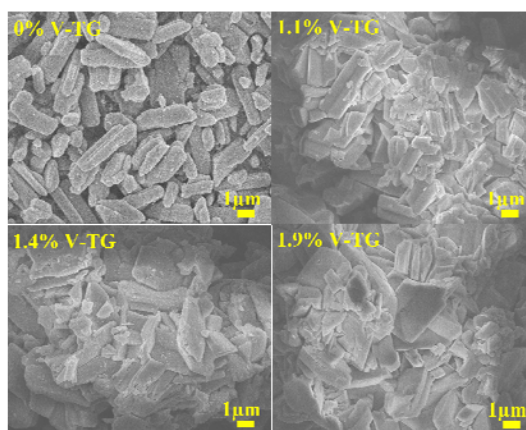


**Fig. S2.** SEM images of V-TG precursors with different vanadium contents.

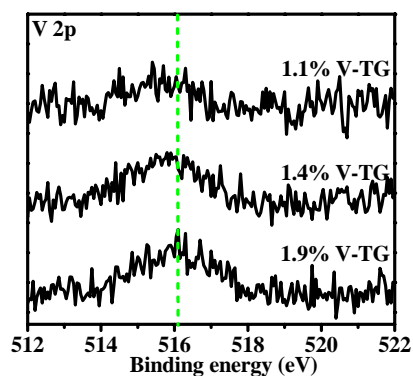


**Fig. S3.** High resolution XPS spectra of V 2p<sub>3/2</sub> for V-TG with different V-doping levels.

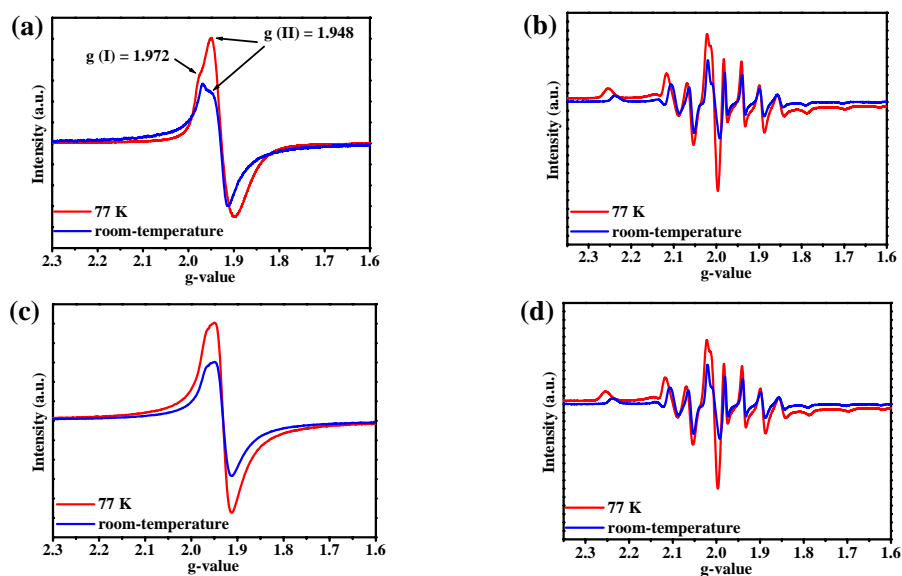


**Fig. S4.** EPR spectra of a) V-TiO<sub>2</sub>(H<sup>\*</sup>) ; b) V-TiO<sub>2</sub>; c) un-doped TiO<sub>2</sub>(H<sup>\*</sup>) and d) V-TG precursor at 77K (red) and room-temperature (blue).

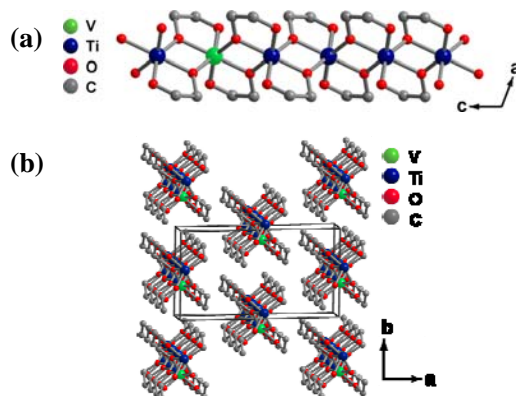


**Fig. S5.** a) Schematic view of the metal alkoxide chains of V-TG precursor along the c axis; b) View of the array of one-dimensional chains in V-TG precursor along the c axis.

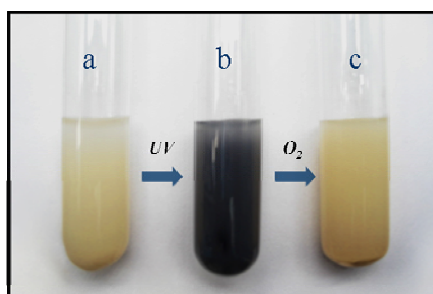


**Fig. S6.** Photos of a) V-TG, b) V-TiO<sub>2</sub>(H<sup>\*</sup>) and c) V-TiO<sub>2</sub>.

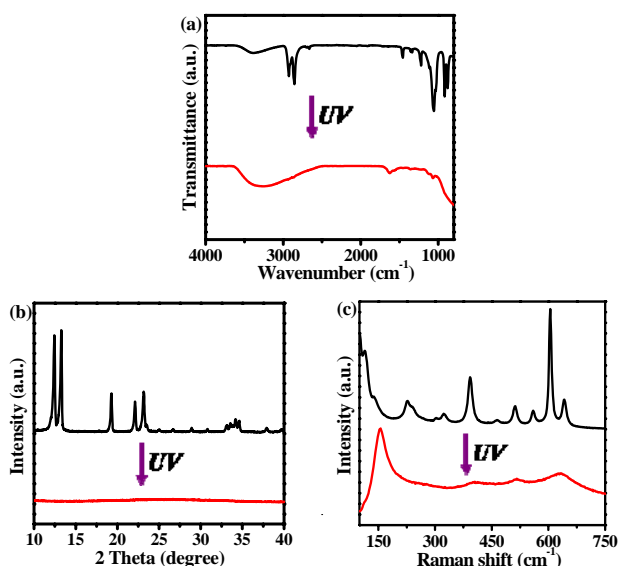


**Fig. S7.** (a) FT-IR spectra, (b) XRD patterns and (c) Raman spectra for 1.4% V-TG (black) and 1.4% V-TiO<sub>2</sub> (red).

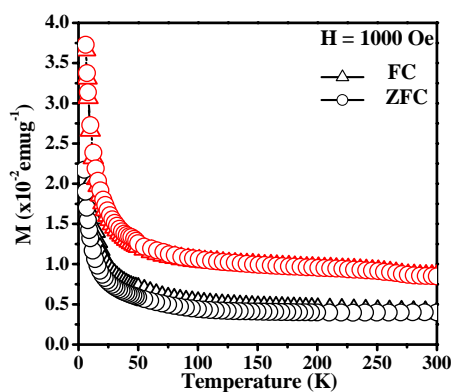


**Fig. S8.** Magnetization as a function of temperature for 0% V-TiO<sub>2</sub>(H\*) (black) and 1.4% V-TiO<sub>2</sub>(H\*) reductants (red) under the zero-field cooled (ZFC) and field-cooled (FC) conditions with  $H = 1000$  Oe. (both paramagnetism and ferromagnetism contribute to the total magnetization of the reductants)

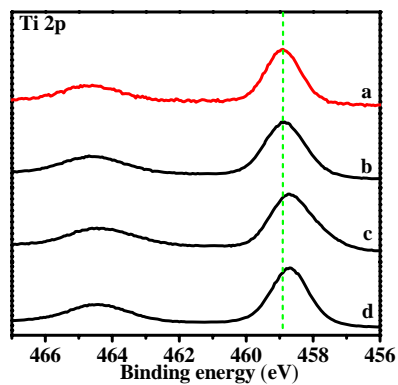


**Fig. S9.** XPS spectra of Ti 2p for a) 0% V-TiO<sub>2</sub>, b) 1.1% V-TiO<sub>2</sub>, c) 1.4% V-TiO<sub>2</sub> and d) 1.9% V-TiO<sub>2</sub>.

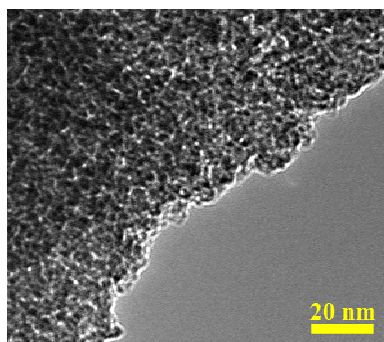


**Fig. S10.** Representative TEM image of 1.4% V-TiO<sub>2</sub>.

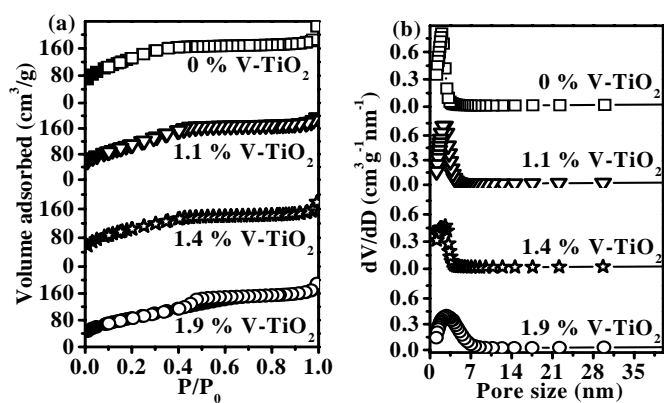


**Fig. S11.** a) N<sub>2</sub> adsorption/desorption isotherms and b) pore-size distribution for V-TiO<sub>2</sub> samples with different vanadium contents.

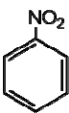
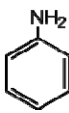
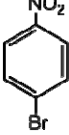
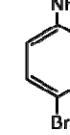
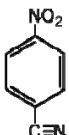
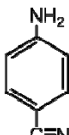
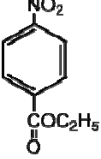
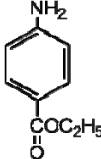
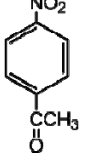
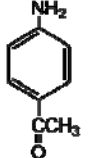
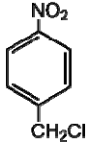
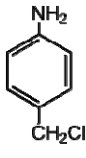
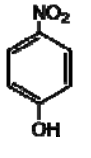
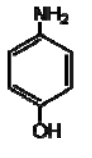
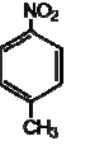
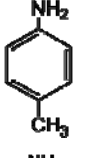
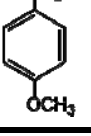
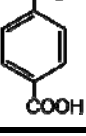
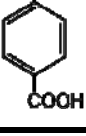
**Table S1.** BET surface area, average pore diameter and proportion of Ti-O-Ti oxygen of the as-prepared V-TiO<sub>2</sub> samples with different vanadium contents.

Sample	BET surface area (m <sup>2</sup> g <sup>-1</sup> )	Average pore diameter (nm)	Proportion of Ti-O-Ti oxygen (%)
0% V-TiO <sub>2</sub>	534	1.8	50.4
1.1% V-TiO <sub>2</sub>	512	2.3	70.8
1.4% V-TiO <sub>2</sub>	484	2.4	75.9
1.9% V-TiO <sub>2</sub>	398	3.0	74.1

**Table S2.** Organic compounds with oxidative or unsaturated groups for the investigation of selective reduction property of V-TiO<sub>2</sub>(H<sup>\*</sup>) reductants.

Series	Organic compounds non-reducible by V-TiO <sub>2</sub> (H <sup>*</sup> )
Aliphatic	
Aromatic	

**Table S3. Chemoselective hydrogenation of nitroarenes to aminoarenes with substituting groups on the para-position by the as-prepared V-TiO<sub>2</sub>(H<sup>\*</sup>) reductants.**

Entry	Substrate	Product	t (s)	Yield (%)	Entry	Substrate	Product	t (s)	Yield (%)
1			<10	>99	6			<10	>99
2			<10	>99	7			<10	>99
3			<10	>99	8			<10	>99
4			<10	>99	9			<10	>99
5			<10	>99	10			<10	>99